Optimization of Bipyridinyl Pyrazole Scaffolds via Design, Synthesis and Screening of a New Series of ROS1 Kinase-modulating Compounds

Mohammad M. Al-Sanea,[†,‡,||] Byung Sun Park,[§,||] Ahmed Z. Abdelazem,[†,‡] Khalid B. Selim,[¶] Kyung Ho Yoo,[‡] Taebo Sim,[‡] Jin Sung Tae,[§] and So Ha Lee[‡,*]

[†]*Department of Biological Chemistry, Korea University of Science and Technology, Daejeon 305-333, Republic of Korea*
[‡]*Chemical Kinomics Research Center, Korea Institute of Science and Technology, Seoul 136-791, Republic of Korea. *E-mail: LSH6211@kist.re.kr*
[§]*Department of Chemistry, Yonsei University, Seoul 120-749, Republic of Korea*
[¶]*Department of Pharmaceutical Organic Chemistry, Faculty of Pharmacy, Mansoura University, Mansoura 35516, Egypt*
Received September 5, 2014, Accepted October 21, 2014, Published online January 5, 2015

A series of rationally designed ROS1 tyrosine kinase inhibitors **6a–9b** with bipyridinyl pyrazole scaffold was synthesized and screened. The scaffold itself has showed an exclusive selectivity profile over ROS1 closely related kinases, ALK and c-Met. The aim of this study was to further explore the structure–activity relationships (SAR) of the bipyridinyl pyrazole core structure, and to improve its ROS1 inhibitory potency. The rational of this study was to explore the nature of the proposed binding site for the pyrazole NH substituents. Careful selections of pyrazole NH substituent groups along with their regioisomers were considered. The compounds exhibited high degree of potency, IC_{50} values of 21–159 nM. A detailed SAR of bipyridinyl pyrazole scaffold has been finally well established and the virtual screening strategy, through molecular docking, has been performed for this type of ROS1 kinase inhibitors and the docked poses along with the activity data have gone in consistent with SAR specifications.

Keywords: ROS1 kinase inhibitor, Bipyridinyl pyrazole, Cancer, Chromosomal alteration

Introduction

Proto-oncogene tyrosine-protein kinase ROS (ROS1) is a receptor tyrosine kinase (RTK). RTKs are transmembrane glycoproteins that mediate signal transduction and cell-to-cell communication. They act as cell surface receptors for a number of important growth factors and hormones.[1–4] However, protein kinase activation by somatic mutation or chromosomal alteration is a key role in the initiation and progression of a number of cancers.[5–8]

ROS1 has become one of the most extensively studied to date, and the ectopic expression as well as the production of variable mutant forms of ROS1 kinase have been reported in a number of cancers, such as glioblastoma multiforme, cholangiocarcinoma, and nonsmall cell lung cancer (NSCLC).[9–14] ROS1 forms fusions and defines another clinically actionable oncogenic driver mutation in NSCLC. Recently, it has been reported that around 1.4% of NSCLCs harbor ROS1 rearrangements.[15,16]

Because of the high homology between the kinase domains of ROS1 and ALK, several ALK inhibitors were assayed against ROS1-driven cells and tumors, and they have demonstrated *in-vitro* inhibitory activity against ROS1.[14,15,17] NVP-TAE684 showed *in-vitro* activity against HCC78 cell lines and inhibition of signaling downstream of ROS1 inducing apoptosis in BaF3/FIG-ROS positive cells (IC_{50} = 10 nM).[14] Crizotinib, first ALK inhibitor approved by FDA, is also able to inhibit ROS1 with an IC_{50} value of 1.7 nM in an *in-vitro* assay. The 2% cases appointed by NSCLC harbor ROS1 rearrangements were totally recovered in 12 weeks after crizotinib treatment.[18]

The phenyl bipyridinyl scaffold, reported by our group, has unleashed several ROS1 kinase inhibitors with IC_{50} range of 13.6–209 nM in enzyme-based screening. Compound KIST301072 showed high degree of selectivity among 45 kinases.[19,20]

Herein, the aim of the study is to further explore the structure–activity relationships (SAR) of the bipyridinyl pyrazole core structure, and to improve its ROS1 inhibitory potency. Therefore, a series of rationally selected derivatives of bipyridinyl pyrazole scaffold were designed by carefully selecting different substituents on pyrazole NH in order to explore their binding role and hence discover the nature of their complementary region of interaction.

Materials and Methods

General Remarks. Commercially available reagents and anhydrous solvents were used without further purification

|| These authors contributed equally to this work.

unless otherwise specified. Thin-layer chromatography (TLC) analyses were performed with precoated (silica gel 60 F254 prepared by E. Merck, Darmstadt, Germany). NMR spectra were recorded with a Bruker 300 MHz spectrometer at ambient temperature with the residual solvent peaks as internal standards. The line positions of multiplets were given in ppm (δ) and the coupling constants (*J*) were given in hertz. Flash chromatography was performed on columns of Merck silica gel (230–400 mesh, 40–63 μm) with ethylacetate/hexane or methanol/dichloromethane as eluents.

2-Chloro-6-(3-(3-methoxy-5-methylphenyl)-1-methyl-1*H*-pyrazol-4-yl)pyridine (4a) and 2-chloro-6-(5-(3-methoxy-5-methylphenyl)-1-methyl-1*H*-pyrazol-4-yl)pyridine (5a): To a mixture of **3** (1 g, 3.34 mmol) and K_2CO_3 (0.92 g, 6.67 mmol) in dimethylformamide (DMF; 10 mL) was added dropwise iodomethane (0.42 mL, 6.67 mmol). The reaction mixture was stirred at room temperature for 3 h and the solvent was evaporated under vacuum. The residue was partitioned between brine and ethyl acetate. The combined organic layers were dried over anhydrous $MgSO_4$ and evaporated under vacuum. The crude product was purified by column chromatography (silica gel, ethyl acetate–hexane) to yield **4a** (0.33 g, 32%, lower spot in TLC) and **5a** (0.22 g, 21%, upper spot in TLC). **4a**: ^{1}H NMR (300 MHz, $CDCl_3$) δ 2.22 (s, 3H), 3.63 (s, 3H), 3.87 (s, 3H), 6.66 (d, *J* = 5.4 Hz, 2H), 6.80 (s, 1H), 6.99 (d, *J* = 4.2 Hz, 1H), 7.17 (s, 1H), 7.53 (s, 1H), 8.12 (d, *J* = 4.8 Hz, 1H); **5a**: ^{1}H NMR (300 MHz, $CDCl_3$) δ 2.29 (s, 3H), 3.68 (d, *J* = 10. 8 Hz, 6H), 6.54 (s, 1H), 6.61 (s, 1H), 6.77 (s, 1H), 6.84 (d, *J* = 4.5 Hz, 1H), 7.08 (s, 1H), 7.73 (s, 1H), 8.03 (d, *J* = 5.1 Hz, 1H).

2-Chloro-6-(1-ethyl-3-(3-methoxy-5-methylphenyl)-1*H*-pyrazol-4-yl)pyridine (4b) and 2-chloro-6-(1-ethyl-5-(3-methoxy-5-methylphenyl)-1*H*-pyrazol-4-yl)pyridine (5b): To a mixture of **3** (1 g, 3.34 mmol) and K_2CO_3 (0.92 g, 6.67 mmol) in a DMF solution (10 mL) was added iodoethane (1.07 mL, 6.67 mmol) dropwise. The reaction mixture was stirred at room temperature for 3 h and the solvent was evaporated under vacuum. The residue was partitioned between brine and ethyl acetate. The combined organic layers were dried over $MgSO_4$ and evaporated under vacuum. The mixture of **4b** and **5b** (0.62 g, 57%) was used in the next step without further purification because of the difficulty of separation.

3-(4-(6-Chloropyridin-2-yl)-3-(3-methoxy-5-methylphenyl)-1*H*-pyrazol-1-yl)propanenitrile (4c) and 3-(4-(6-chloropyridin-2-yl)-5-(3-methoxy-5-methyl phenyl)-1*H*-pyrazol-1-yl)propanenitrile (5c): To a mixture of **3** (1 g, 3.34 mmol) and K_2CO_3 (0.92 g, 6.67 mmol) in DMF solution (10 mL) was added 3-iodopropionitrile (0.6 mL, 6.67 mmol) dropwise. The reaction mixture was stirred at room temperature for 3 h and the solvent was evaporated under vacuum. The residue was partitioned between brine and ethyl acetate. The combined organic layers were dried over anhydrous $MgSO_4$ and evaporated under vacuum. The mixture of **4c** and **5c** (0.94 g, 80%) was used in the next step without further purification because of the difficulty of separation.

2-(4-(6-Chloropyridin-2-yl)-3-(3-methoxy-5-methyl phenyl)-1*H*-pyrazol-1-yl)acetamide (4d): To a mixture of **3** (1 g, 3.34 mmol) and K_2CO_3 (0.92 g, 6.67 mmol) in DMF solution (10 mL) was added 2-iodoacetamide (1.24 g, 6.67 mmol). The reaction mixture was stirred at room temperature for 3 h and the solvent was evaporated under vacuum. The residue was partitioned between brine and ethyl acetate. The combined organic layers were dried over anhydrous $MgSO_4$ and evaporated under vacuum to yield the pure product **4d** (1.1 g, 92%); ^{1}H NMR (300 MHz, CD_3OD) δ 3.08 (s, 3H), 4.50 (s, 3H), 5.66 (s, 2H), 7.70–7.48 (m, 3H), 8.03 (d, *J* = 5.1 Hz, 1H), 8.14 (d, *J* = 13.2 Hz, 1H), 9.10–8.96 (m, 2H).

4-(3-(3-Methoxy-5-methylphenyl)-1-methyl-1*H*-pyrazol-4-yl)-2,3′-bipyridine (6a): A mixture of **4a** (172 mg, 0.55 mmol), 3-pyridineboronic acid (81 mg, 0.66 mmol), dichlorobis(triphenylphosphine)Pd(II) (12 mg, 0.017 mmol) and K_2CO_3 (76 mg, 0.55 mmol) was placed in a mixed solvent of acetonitrile and water (4:1, 5 mL). N_2 gas was bubbled into this mixture for 15 min, and then the mixture was refluxed while stirring under N_2 atmosphere for 1 h. The reaction mixture was cooled to room temperature, and then poured into ice water and extracted with ethyl acetate. The combined organic layers were washed with brine, dried over anhydrous $MgSO_4$, and evaporated under vacuum. The crude product was purified by column chromatography (silica gel, ethyl acetate) to yield the pure product **6a** (133 mg, 68%); ^{1}H NMR (300 MHz, $CDCl_3$) δ 2.24 (s, 3H), 3.64 (s, 3H), 3.93 (s, 3H), 6.68 (s, 1H), 6.75 (s, 1H), 6.88 (s, 1H), 7.13 (d, *J* = 4.2 Hz, 1H), 7.3 (d, *J* = 4.1 Hz, 1H), 7.6 (d, *J* = 9.6 Hz, 2H), 8.14 (d, *J* = 7.8 Hz, 1H), 8.51–8.56 (m, 2H), 8.94 (s, 1H); positive ion ESI-MS *m*/*z* 379.1632 $(M + Na)^+$.

4-(5-(3-Methoxy-5-methylphenyl)-1-methyl-1*H*-pyrazol-4-yl)-2,3′-bipyridine (7a): A mixture of **5a** (88 mg, 0.37 mmol), 3-pyridineboronic acid (55 mg, 0.44 mmol), dichlorobis(triphenylphosphine)Pd(II) (8 mg, 0.011 mmol) and K_2CO_3 (51 mg, 0.37 mmol) was placed in a mixed solvent of acetonitrile and water (4:1, 5 mL). N_2 gas was bubbled into this mixture for 15 min, and then the mixture was refluxed while stirring under N_2 atmosphere for 1 h. The reaction mixture was cooled to room temperature, and then poured into ice water and extracted with ethyl acetate. The combined organic layers were washed with brine, dried over anhydrous $MgSO_4$, and evaporated under vacuum. The crude product was purified by column chromatography (silica gel, ethyl acetate) to yield the pure product **7a** (88 mg, 66%); ^{1}H NMR (300 MHz, $CDCl_3$) δ 2.33 (s, 3H), 3.73 (s, 6H), 6.62 (s, 1H), 6.70 (s, 1H), 6.84 (s, 1H), 7.06 (d, *J* = 5.1 Hz, 1H), 7.3 (t, *J* = 6.0 Hz, 1H), 7.45 (s, 1H), 7.83 (s, 1H), 8.12 (d, *J* = 7.5 Hz, 1H), 8.45 (d, *J* = 5.1 Hz, 1H), 8.54 (d, *J* = 3.9 Hz, 1H), 8.80 (s, 1H); positive ion ESI-MS *m*/*z* 379.1542 $(M + Na)^+$.

4-(1-Ethyl-3-(3-methoxy-5-methylphenyl)-1*H*-pyrazol-4-yl)-2,3′-bipyridine (6b) and 4-(1-ethyl-5-(3-methoxy-5-methylphenyl)-1*H*-pyrazol-4-yl)-2,3′-bipyridine (7b): A mixture of **4b** and **5b** (0.62 g, 1.89 mmol), 3-pyridineboronic acid (0.28 g, 2.27 mmol), dichlorobis (triphenylphosphine)Pd(II) (40 mg, 0.057 mmol) and K_2CO_3 (0.39

g, 2.84 mmol) was placed in a mixed solvent of acetonitrile and water (4:1, 5 mL). N_2 gas was bubbled into this mixture for 15 min, and then the mixture was refluxed while stirring under N_2 atmosphere for 1 h. The reaction mixture was cooled to room temperature, and then poured into ice water and extracted with ethyl acetate. The combined organic layers were washed with brine, dried over anhydrous $MgSO_4$, and evaporated under vacuum. The mixture of **6b** and **7b** (0.45 g, 65%) was used for the next step without further purification because of the difficulty of separation.

3-(4-([2,3′-Bipyridin]-4-yl)-3-(3-methoxy-5-methylphenyl)-1*H*-pyrazol-1-yl)propanenitrile (6c) and 3-(4-([2,3′-bipyridin]-4-yl)-5-(3-methoxy-5-methylphenyl)-1*H*-pyrazol-1-yl)propanenitrile (7c): A mixture of **4c** and **5c** (0.9 g, 2.55 mmol), 3-pyridineboronic acid (0.38 g, 3.06 mmol), dichlorobis(triphenylphosphine)Pd(II) (54 mg, 0.077 mmol) and K_2CO_3 (0.53 g, 3.83 mmol) was placed in a mixed solvent of acetonitrile and water (4:1, 5 mL). N_2 gas was bubbled into this mixture for 15 min, and then the mixture was refluxed while stirring under N_2 atmosphere for 1 h. The reaction mixture was cooled to room temperature, and then poured into ice water and extracted with ethyl acetate. The combined organic layers were washed with brine, dried over anhydrous $MgSO_4$, and evaporated under vacuum. The crude product was purified by column chromatography (silica gel, ethyl acetate-hexane) to yield **6c** and **7c** (0.37 g, 37%, upper spot in TLC). **6c**: mp 59–61 °C; ^{1}H NMR (300 MHz, $CDCl_3$) δ 2.32 (s, 3H), 3.07 (t, J = 4.8 Hz, 2H), 3.72 (s, 3H), 4.48 (t, J = 5.0 Hz, 2H), 6.78 (d, J = 0.5 Hz, 1H), 6.83 (t, J = 1.2 Hz, 1H), 6.94 (d, J = 0.3 Hz, 1H), 7.21 (dd, J = 1.2, 3.9 Hz, 1H), 7.39–7.36 (m, 1H), 7.66 (d, J = 0.6 Hz, 1H), 7.84 (s, 1H), 8.21 (dt, J = 1.1, 5.5 Hz, 1H), 8.63–8.60 (m, 2H), 9.02 (d, J = 1.5 Hz, 1H); ^{13}C NMR (75 MHz, $CDCl_3$) δ 19.42, 21.54, 47.97, 55.27, 111.12, 115.34, 116.95, 118.57, 121.75, 121.81, 123.66, 130.40, 133.36, 134.56, 134.92, 140.00, 141.65, 147.97, 149.69, 150.18, 151.08, 154.83, 159.77; **7c**: mp 125–127 °C; ^{1}H NMR (300 MHz, $CDCl_3$) δ 2.44 (d, J = 0.3 Hz, 3H), 3.00 (t, J = 4.9 Hz, 2H), 3.85 (s, 3H), 4.32 (t, J = 5.0 Hz, 2H), 6.78 (t, J = 1.2 Hz, 1H), 6.84 (d, J = 0.6 Hz, 1H), 6.98 (q, J = 0.6 Hz, 1H), 7.16 (dd, J = 1.2, 3.9 Hz, 1H), 7.29 (s, 1H), 7.43 (dd, J = 3.8, 5.8 Hz, 1H), 7.56 (q, J = 0.6 Hz, 1H), 8.02 (s, 1H), 8.26 (dt, J = 1.5, 6.1 Hz, 1H), 8.57 (dd, J = 0.6 and 3.9 Hz, 1H), 8.66 (d, J = 3.0 Hz, 1H), 8.91 (s, 1H); ^{13}C NMR (75 MHz, $CDCl_3$) δ 18.81, 29.72, 44.58, 55.55, 112.86, 116.45, 116.87, 118.17, 120.53, 122.89, 124.02, 129.69, 135.51, 138.81, 141.39, 142.23, 146.84, 148.70, 149.95, 160.49.

2-(4-([2,3′-Bipyridin]-4-yl)-3-(3-methoxy-5-methylphenyl)-1*H*-pyrazol-1-yl)acetamide (6d): A mixture of **4d** (100 mg, 0.28 mmol), 3-pyridineboronic acid (41 mg, 0.34 mmol), dichlorobis(triphenylphosphine)Pd(II) (6 mg, 0.008 mmol) and K_2CO_3 (39 mg, 0.28 mmol) was placed in a mixed solvent of acetonitrile and water (4:1, 5 mL). N_2 gas was bubbled into this mixture for 15 min, and then the mixture was refluxed while stirring under N_2 atmosphere for 1 h. The reaction mixture was cooled to room temperature, and then poured into ice water and extracted with ethyl acetate. The combined organic layers were washed with brine, dried over anhydrous $MgSO_4$, and evaporated under vacuum. The crude product was purified by column chromatography (silica gel, ethyl acetate) to yield the pure product **6d** (50 mg, 45%); mp 206–208 °C; ^{1}H NMR (300 MHz, DMSO-d_6) δ 2.52 (s, 3H), 3.69 (s, 3H), 4.88 (s, 2H), 6.78 (d, J = 0.9 Hz, 1H), 6.82 (d, J = 0.6 Hz, 1H), 6.91 (d, J = 0.6 Hz, 1H), 7.24 (dd, J = 1.2, 3.9 Hz, 1H), 7.39 (s, 1H), 7.54–7.50 (m, 1H), 7.66 (s, 1H), 7.94 (d, J = 0.6 Hz, 1H), 8.36–8.33 (m, 1H), 8.37 (s, 1H), 8.59 (dd, J = 0.3, 3.9 Hz, 1H), 8.64 (dd, J = 1.2, 3.6 Hz, 1H), 9.13 (q, J = 0.7 Hz, 1H); ^{13}C NMR (75 MHz, DMSO) δ 21.56, 54.56, 55.45, 111.42, 114.87, 117.41, 119.38, 121.75, 121.90, 124.23, 133.69, 134.34, 134.67, 139.69, 142.38, 148.14, 148.90, 150.37, 150.43, 154.51, 159.68, 168.70.

3-(4-([2,3′-Bipyridin]-4-yl)-1-methyl-1*H*-pyrazol-3-yl)-5-methylphenol (8a): To a solution of **6a** (99 mg, 0.28 mmol) in dichloromethane (5 mL) was added borontrifluoride–dimethylsulfide complex (568 μL, 2.8 mmol) dropwise at room temperature under N_2 atmosphere. The resulting suspension was stirred at room temperature for 12 h and the reaction mixture was concentrated under reduced pressure. The residue was partitioned between water and ethyl acetate. The combined organic layers were dried over $MgSO_4$ and evaporated under vacuum. The crude product was purified by column chromatography (silica gel, ethyl acetate) to yield the pure product **8a** (60 mg, 63%); ^{1}H NMR (300 MHz, $CDCl_3$) δ 2.15 (s, 3H), 3.85 (s, 3H), 6.5–6.81 (m, 3H), 7.07 (d, J = 4.8 Hz, 1H), 7.19–7.23 (m, 1H), 7.51 (d, J = 14.1 Hz, 2H), 8.06 (d, J = 7.8 Hz, 1H), 8.36 (dd, J = 5.1, 4.5 Hz, 2H), 8.72 (d, J = 7.5 Hz, 1H); positive ion ESI-MS m/z 343.1559 $(M + H)^+$.

3-(4-([2,3′-Bipyridin]-4-yl)-1-methyl-1*H*-pyrazol-5-yl)-5-methylphenol (9a): To a solution of **7a** (80 mg, 0.22 mmol) in dichloromethane (5 mL) was added borontrifluoride–dimethylsulfide complex (455 μL, 2.2 mmol) dropwise at room temperature under N_2 atmosphere. The resulting suspension was stirred at room temperature for 12 h and the reaction mixture was concentrated under reduced pressure. The residue was partitioned between water and ethyl acetate. The combined organic layers were dried over anhydrous $MgSO_4$ and evaporated under vacuum. The crude product was purified by column chromatography (silica gel, ethyl acetate) to yield the pure product **9a** (55 mg, 73%); ^{1}H NMR (300 MHz, $CDCl_3$) δ 2.28 (s, 3H), 3.75 (s, 3H), 6.62 (d, J = 9.6 Hz, 2H), 6.90 (s, 1H), 7.19 (s, 3H), 7.38 (s, 2H), 7.819 (s, 1H), 8.29 (d, J = 7.8 Hz, 1H), 8.45 (d, J = 5.1 Hz, 1H); positive ion ESI-MS m/z 365.1389 $(M + Na)^+$.

3-(4-([2,3′-Bipyridin]-4-yl)-1-ethyl-1*H*-pyrazol-3-yl)-5-methylphenol (8b) and 3-(4-([2,3′-bipyridin]-4-yl)-1-ethyl-1*H*-pyrazol-5-yl)-5-methylphenol (9b): To a solution of **6b** and **7b** (0.26 g, 0.7 mmol) in dichloromethane (5 mL) was added borontrifluoride–dimethylsulfide complex (1.4 mL, 7 mmol) dropwise at room temperature under N_2 atmosphere. The resulting suspension was stirred at room temperature for 12 h and the reaction mixture was concentrated under

reduced pressure. The residue was partitioned between water and ethyl acetate. The combined organic layers were dried over anhydrous $MgSO_4$ and evaporated under vacuum. The crude product was purified by preparative TLC (silica gel, toluene–MeOH–AcOH–acetone, 1:1:0.25:0.25, v/v/v/v) to yield **8b** (32 mg, 13%, lower spot in TLC) and **9b** (22 mg, 9%, upper spot in TLC). **8b**: ^{1}H NMR (300 MHz, $CDCl_3$) δ 1.48 (t, J = 7.2 Hz, 3H), 2.17 (s, 3H), 4.16 (q, J = 7.2 Hz, 2H), 6.57 (s, 1H), 6.70 (s, 1H), 6.84 (s, 1H), 7.11–7.13 (m, 1H), 7.26 (q, J = 4.3 Hz, 1H), 7.52 (s, 1H), 7.60 (s, 1H), 8.11 (d, J = 7.8 Hz, 1H), 8.4 (d, J = 5.1 Hz, 2H), 8.75 (s, 1H), 9.61 (s, 1H); **9b**: ^{1}H NMR (300 MHz, $CDCl_3$) δ 1.44 (t, J = 7.35, 3H), 2.39 (s, 3H), 4.15 (q, J = 7.1 Hz, 2H), 7.3 (d, J = 4.2 Hz, 1H), 6.93 (s, 1H), 7.24 (d, J = 5.1 Hz, 1H), 7.48–7.57 (m, 2H), 7.94 (s, 1H), 8.12 (s, 2H), 8.26 (t, J = 6.3 Hz, 1H), 8.55 (d, J = 5.1 Hz), 8.74 (s, 1H).

ROS1 Kinase Assays. The compounds were screened by the same method in the literature.[20]

Molecular Modeling. The compounds were studied by the same method in the literature.[20]

Results and Discussion

The preparation of compounds **6–9** is outlined in Scheme 1. A nucleophilic substitution reaction using lithium hexamethyldisilazide (LHMDS) was selected for attacking a benzoate ester **1** by 2-chloro-4-methylpyridine. The nucleophile was produced *in situ* by abstracting one proton of the methyl group via dropwise addition of LHMDS in dry THF at ambient temperature, which in turn converts 4-methyl group into an active methylene, and achieved the adduct with a mixture of keto and enol tautomers **2**.

The conversion of the resulted tautomers **2** to the required pyrazole **3** was achieved through two successive steps. In the first step, compound **2** was heated with excess *N,N*-dimethylformamide dimethylacetal for 12 h, and the resulted product was taken to the next step without further purification, where it was cyclized with hydrazine monohydrate in absolute ethanol into the pyrazole derivative **3** as reported.[21] The reaction of the resulted pyrazole **3** with 4 different alkyl iodides in the presence of excess potassium carbonate produced two different regioisomers, compounds **4a–d** and **5a–d**.

The structures of 1*H*-pyrazole and its regioisomer, 2*H*-pyrazole were confirmed before by the two-dimensional Nuclear Overhauser effect spectroscopy (NOESY) NMR spectrum.[19] Generally, the 1*H*-pyrazole isomer was the product with the lower R_f at which the CH_2 protons of the NH substituent group exhibited NOE interactions with two ortho aromatic protons at carbon 2 and 6. However, the second 2*H*-pyrazle isomer was the product with the higher R_f and does not show any cross peak between the CH_2 protons of the NH substituent group and any of the aromatic protons of 3-methoxy-5-methylphenyl group. The distance factor is the sole factor for making the CH_2 proton being accessible or not for making spatial coupling with the two ortho aromatic protons. Furthermore, the anticipated higher shielding of the two protons of the NH substituent CH_2 in all of the 2*H*-pyrazole isomers caused by the anisotropic effect of the nearby aromatic

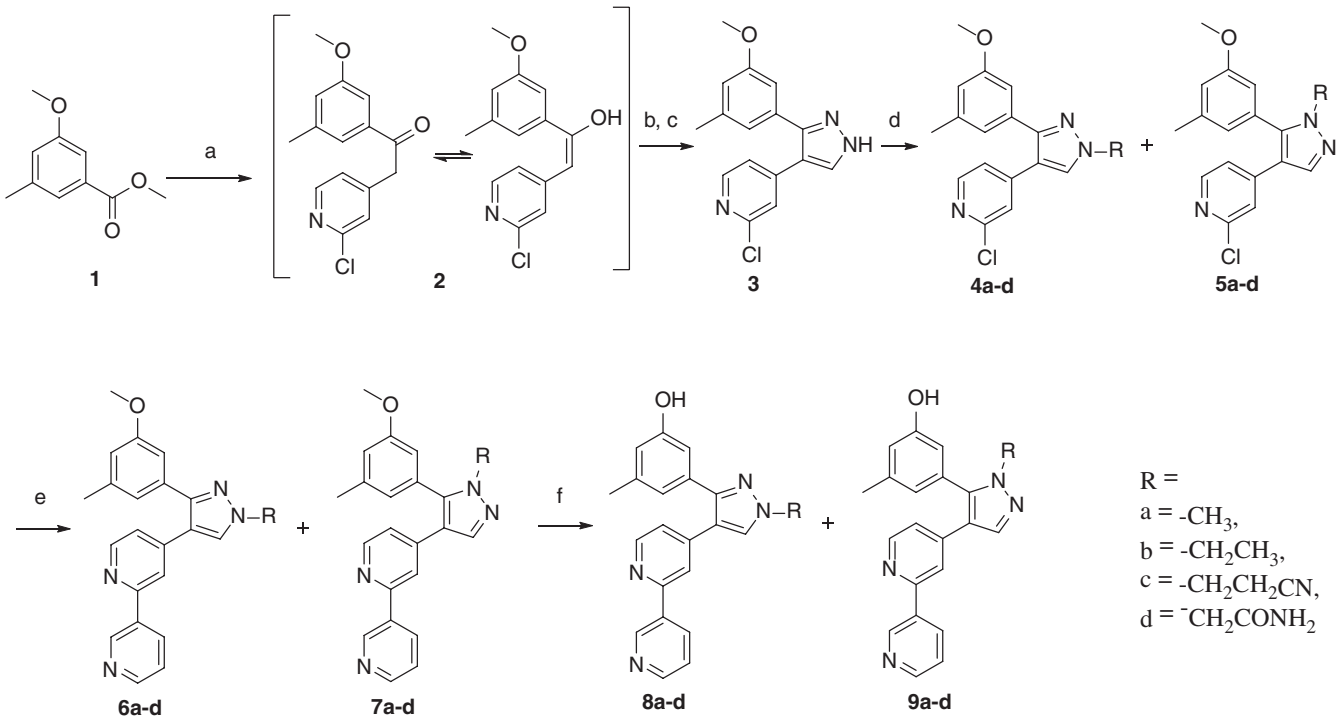

Scheme 1. Reaction conditions and reagents: (a) LHMDS, 2-chloro-4-methylpyridine, THF, N_2, room temperature (rt), 24 h, 72%; (b) DMF-DMA, 90 °C, 12 h; (c) $NH_2NH_2{\cdot}H_2O$, abs. EtOH, rt, 2 h, 81%; (d) K_2CO_3, RI, DMF, rt, 3 h; (e) 3-pyridineboronic acid, $Pd(PPh_3)_2Cl_2$, K_2CO_3, N_2, CH_3CN/H_2O (4/1), reflux, 1 h; (f) $BF_3{\cdot}S(CH_3)_2$, CH_2Cl_2, N_2, rt, 24 h.

electron cloud, was proved also before and in the experimental section as the ^{1}H NMR spectra of two pairs of compounds **6c**, **7c** and **8b, 9b**. In the 2*H*-isomers, such protons appeared at upfield δ values; however in the 1*H*-isomers, these protons were more downfield shifted.

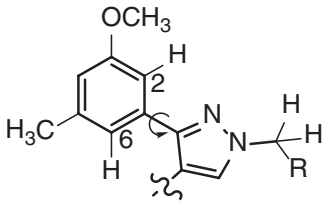

***1H*-pyrazole**

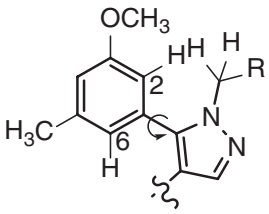

***2H*-pyrazole**

Then Suzuki coupling of compound **4a–d** and **5a–d** with 3-pyridineboronic acid, in the presence of dichlorobis(triphenylphosphine)Pd(II) and potassium carbonate, in a mixed solvent of acetonitrile and water in a ratio (4:1), produced compounds **6a–d** and **7a–d**, respectively. The corresponding hydroxyl products **8a–d** and **9a–d** were obtained by demethylation of the methoxy group of compounds **6a–d** and **7a–d** using 10 equiv of borontrifluoride–dimethylsulfide complex in dichloromethane.

Kinase assays were performed at Reaction Biology Corporation using the "HotSpot" assay platform.[20] In the initial screening step of the synthesized compounds, the compounds were tested over ROS1 kinase at a single dose of 20 μM, and the reaction was carried out at 10 μM ATP concentration.

After long term of handling bipyridinyl pyrazole as a core structure with good ROS1 inhibitory potency, the binding mode and the detailed roles of all scaffold structural features have become well known except the pyrazole moiety and its NH substituents. Herein, the exact binding mode of pyrazole NH substituents has been also clarified and emphasized.

Previously, SAR data analysis has been disclosed after discovering some potent ROS1 kinase inhibitors and the detailed SAR profile has been well understood. Isosteric replacement of distal pyridine with phenyl moiety in some reported compounds harboring the same skeleton has proven the role of distal pyridine N atom as an essential complementary group of hinge residue, methionine Met2029.[21] However, internal pyridine or pyrimidine moieties does not have any binding role with hinge-interacting residues. Furthermore, ortho-substitution of distal pyridine will deteriorate the activity as it sterically hinders the pyridine N from approaching hinge residues and forming the essential hydrogen bond with Met2029. Also, simple deviation in the position of this terminal pyridyl group in space caused by shift in its position from the meta-position to the para-position relative to the central pyridine, results in a great loss of activity too, and this confirms the importance of keeping the orientation of the terminal pyridyl group (Figures 1 and 2).[19,21]

Further SAR studies were then undertaken. The biological screening data have revealed that the pyrazole moiety was essential for ROS1 kinase inhibitory activity, aliphatic replacements of the pyrazole moiety, resulting in inactive compound.[22] Pyrazole ring has an important role in directing both phenyl and the internal pyridine ring toward their complementary sites of interaction at ATP-binding pocket. With regard to the pyrazole NH substitution, distal pyrazole NH is more favorable for substitution, as in compounds **6a–d**, **8a**, and **8b**, than their regioisomers, compounds **7a**, **7c**, **9a and 9b**.

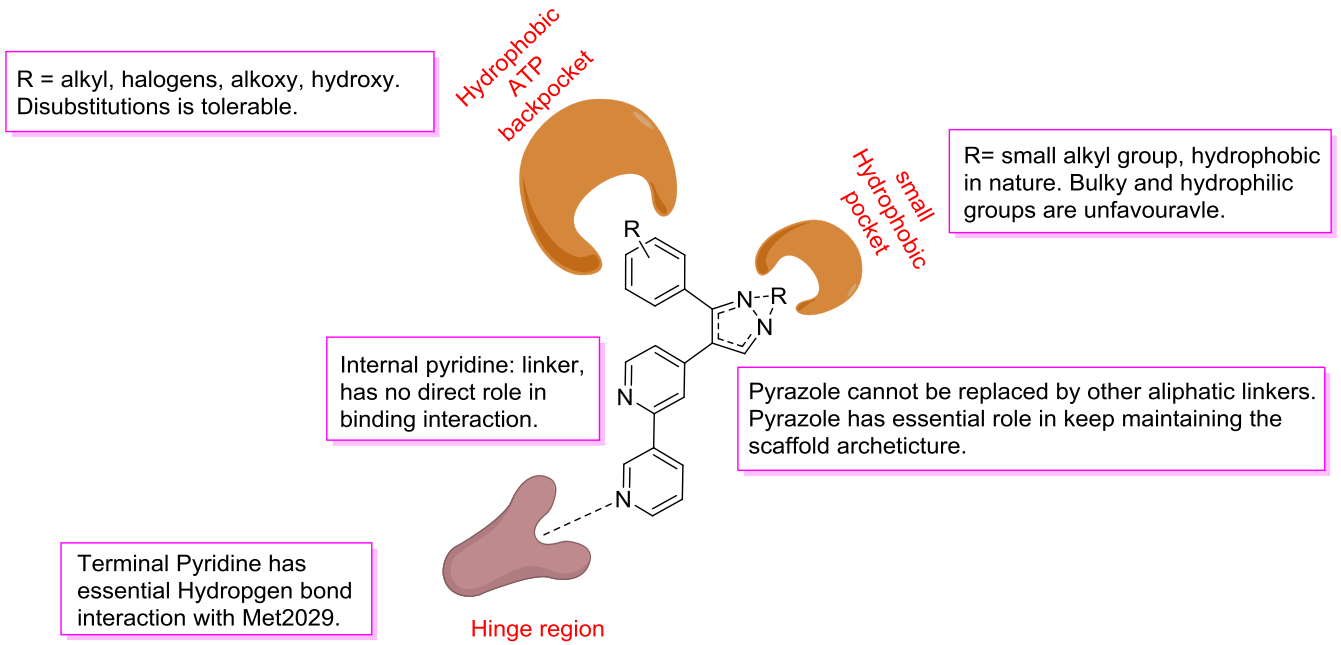

Figure 1. Two-dimensional interaction scheme of bipyridinyl pyrazole scaffold in ROS1 receptor. SARs are illustrated in brief according to pink-colored squares. Hydrogen bonds are shown as dotted lines.

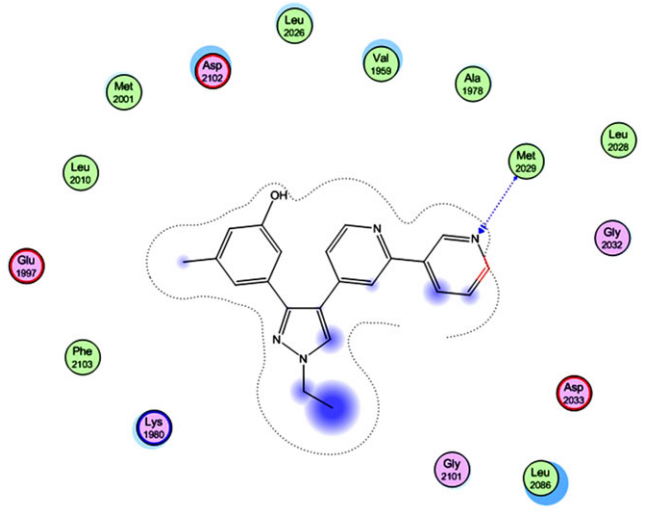

Figure 2. Hydrogen bonding interaction between terminal pyridine of compound **8b** and hinge Met2029.

Distal pyrazole NH substitutions can closely direct the substituent group toward the intended small hydrophobic pocket. The effect of this regioisomerism quietly appears with ethyl and cyanoethyl groups that show significant improvements in potency with 2.5- and 2-folds, respectively (Table 1). The hydrophobic nature of amino acids forming pocket around the pyrazole ring has positive discrimination toward hydrophobic groups being attached to the pyrazole NH moiety. Therefore, groups such as methyl, ethyl, and cyanoethyl groups have revealed magnificent binding interactions as shown in Table 1.

On contrary, pyrazole NH substituent groups with polar hydrophilic nature does not show such kind of potent inhibitory activity as shown by IC_{50} values for **6d**. The phenolic hydroxyl group and its methyl ether have yet undisclosed effect in influencing the inhibitory activity on ROS1 protein.

In case of compounds **6a** and **8a**, the methoxy analog **8a** showed more potency than its hydroxy analog **6a**. However, the hydroxy analog **9a** showed more potent activity than its methoxy analog **7a**.

With regard to the selectivity profile, six compounds have been screened against ROS1 closely related and often crossly inhibited kinases, ALK and c-Met. The results exhibit good ROS1 selectivity profile over them that are considering a new tool in the field of discovering ROS1 kinase inhibitor. Table 1 illustrates how much the improvement in the IC_{50} is going in consistent with the aforementioned points of SAR profile plus the selectivity pattern of six compounds over c-MET and ALK kinases

By investigating the docking mode of compound **8b** using Molecular Operating Environment (MOE) software (2008.10 version, Chemical Computing Group, Inc., Montreal, Quebec, Canada) it has become clear that the nitrogen of the internal pyridine does not share any hydrogen bonding in the receptor; however, the terminal pyridine binds through hydrogen bond with hinge region residue, Met 2029. Figure 3

Table 1. Enzymatic assay results of compounds against kinases.

Comp. No.	R	ROS1 IC_{50} (nM)	ALK IC_{50} (μM)	c-Met IC_{50} (μM)
6a	CH_3	23.2	19.9	20<
6c	CH_2CH_2CN	40	—[a]	—
6d	CH_2CONH_2	159	—	—
7a	CH_3	31.1	17.5	20<
7c	CH_2CH_2CN	74	—	—
8a	CH_3	35	16.4	20<
8b	CH_2CH_3	28.1	20<	20<
9a	CH_3	21	10.8	15.6
9b	CH_2CH_3	79.5	20<	20<
Crizotinib		1.7 (Ref. 23)	0.024 (Ref. 24)	0.011

[a] Not determined.

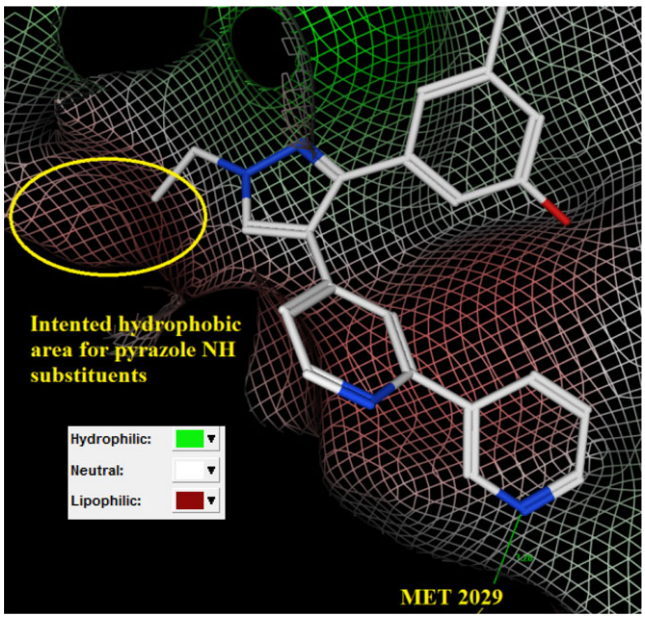

Figure 3. Docking mode of representative ROS1 inhibitors **8b** bound to the ATP-binding pocket of ROS1 protein.[13] It shows key H-bond interaction with hinge residue. The binding motif **8b** shows how much the ethyl group is closely approaching to its complementary hydrophobic area. The convex surface of this area hinders more bulky groups from approaching.

shows a hydrophobic area, with convex surface, which has a steric clash possibility with any bulky group attached to pyrazole NH group. It has become also obvious how the IC_{50} data of final compounds be in consistent with the nature of pyrazole NH substituent groups regarding hydrophobicity and size. Also, we can conclude that the 2H-pyrazole isomer does not support orienting pyrazole NH substituent groups to their intended hydrophobic area. This is because of the possible steric clash between the substituent groups and the receptor surface. Therefore, positive discrimination revealed by hydrophobic area toward pyrazole NH substituent group has become understandable and the observations were consistent with the screening results of all compounds.

Compound **6a** was selected as a representative member of this series to be tested for its the human Ether-à-go-go-Related Gene (hERG) affinity. The results have shown low hERG blockage activity. Compound **6a** binds to the hERG channel with percentage inhibition value of 33.9 at 10 μM. Therefore, this scaffold could be considered as safe scaffold with regard to its potential cardiotoxic activity.

Conclusion

Compounds **6a–9b** were synthesized and screened against ROS1 kinase. Proper selection of substituents, site selection for substitution, avoiding any possible steric clash with important binding regions in ATP-binding site, and fulfilling of all binding requirements on scaffold structure would effectively furnish a lot of potent ROS1 kinase inhibitors, and it has become a novel fertile area for getting out promising candidates in the treatment of ROS1-implicated malignancies. The molecular modeling study has showed the three essential SAR features of phenyl bipyridyl pyrazole core structure. The pyrazole NH substituent groups should be small and hydrophobic in order to fit well with their complementary hydrophobic area.

Acknowledgments. We are grateful to Korea Institute of Science and Technology for supporting the research (2E22760), and this research was supported by a grant (NRF-2011-0028676) from the creative/challenging research program of National Research Foundation of Korea. We also appreciate Reaction Biology Corporation for kinase screening.

References

1. M. A. Alaoui-Jamali, *Biomed. Pharmacother.* **2006**, *60*, 629.
2. A. Chase, N. C. P. Cross, *Clin. Sci.* **2006**, *111*, 233.
3. R. Perona, *Clin. Transl. Oncol.* **2006**, *8*, 77.
4. S. R. Hubbard, W. T. Miller, *Curr. Opin. Cell Biol.* **2007**, *19*, 117.
5. R. Gupta, C. L. Knight, B. J. Bain, *Br. J. Haematol.* **2002**, *117*, 489.
6. Y. Chalandon, J. Schwaller, *Haematologica* **2005**, *90*, 949.
7. E. Lengyel, K. Sawada, R. Salgia, *Curr. Mol. Med.* **2007**, *7*, 77.
8. L. V. Sequist, T. J. Lynch, *Annu. Rev. Med.* **2008**, *59*, 429.
9. L. Nagarajan, E. Louie, Y. Tsujimoto, P. C. Balduzzi, K. Huebner, C. M. Croce, *Proc. Natl. Acad. Sci. U.S.A.* **1986**, *83*, 6568.
10. H. Matsushime, L. H. Wang, M. Shibuya, *Mol. Cell. Biol.* **1986**, *6*, 3000.
11. C. Birchmeier, S. Sharma, M. Wigler, *Proc. Natl. Acad. Sci. U.S.A.* **1987**, *84*, 9270.
12. I. M. El-Deeb, K. H. Yoo, S. H. Lee, *Med. Res. Rev.* **2010**, *31*, 794.
13. M. M. Awad, R. Katayama, M. McTigue, W. Liu, Y.-L. Deng, A. Brooun, L. Friboulet, D. Huang, M. D. Falk, S. Timofeevski, K. D. Wilner, E. L. Lockerman, T. M. Khan, S. Mahmood, J. F. Gainor, S. R. Digumarthy, J. R. Stone, M. Mino-Kenudson, J. G. Christensen, A. J. Iafrate, J. A. Engelman, A. T. Shaw, *New Engl. J. Med.* **2013**, *368*, 2395.
14. S. H. Ou, J. Tan, Y. Yen, R. A. Soo, *Expert Rev. Anticancer Ther.* **2012**, *12*, 447.
15. K. Bergethon, A. T. Shaw, S. H. Ou, R. Katayama, C. M. Lovly, N. T. McDonald, P. P. Massion, C. Siwak-Tapp, A. Gonzalez, R. Fang, E. J. Mark, J. M. Batten, H. Chen, K. D. Wilner, E. L. Kwak, J. W. Clark, D. P. Carbone, H. Ji, J. A. Engelman, M. Mino-Kenudson, W. Pao, A. J. J. Iafrate, *Clin. Oncol.* **2012**, *30*, 863.
16. K. Takeuchi, M. Soda, Y. Togashi, R. Suzuki, S. Sakata, S. Hatano, R. Asaka, W. Hamanaka, H. Ninomiya, H. Uehara, C. Y. Lim, Y. Satoh, S. Okumura, K. Nakagawa, H. Mano, Y. Ishikawa, *Nat. Med.* **2012**, *18*, 378.
17. R. P. Bellacasa, N. Karachaliou, R. Estrada-Tejedor, J. Teixidó, C. Costa, J. I. Borrell, *Transl. Lung Cancer Res.* **2013**, *2*, 72.
18. C. M. Lovly, J. M. Heuckmann, E. de Stanchina, H. Chen, R. K. Thomas, C. Liang, W. Pao, *Cancer Res.* **2011**, *71*, 4920.
19. B. S. Park, I. M. El-Deeb, K. H. Yoo, C. H. Oh, S. J. Cho, D. K. Han, H. S. Lee, J. Y. Lee, S. H. Lee, *Bioorg. Med. Chem. Lett.* **2009**, *19*, 4720.
20. B. S. Park, M. M. Al-Sanea, A. Z. Abdelazem, H. M. Park, E. J. Roh, H.-M. Park, K. H. Yoo, T. Sim, J. S. Tae, S. H. Lee, *Bioorg. Med. Chem.* **2014**, *22*, 3871.
21. I. M. El-Deeb, B. S. Park, S. J. Jung, K. H. Yoo, C. H. Oh, S. J. Cho, D. K. Han, J. Y. Lee, S. H. Lee, *Bioorg. Med. Chem. Lett.* **2009**, *19*, 5622.
22. Abdelazem, A. Z.; Lee, S. H.; *J. Enzyme Inhib. Med. Chem.* Published online 17 June 2014.
23. S. J. Rodig, G. I. Shapiro, *Curr. Opin. Investig. Drugs* **2010**, *11*, 1477.
24. H. Y. Zou, Q. Li, J. H. Lee, M. E. Arango, S. R. McDonnell, S. Yamazaki, T. B. Koudriakova, G. Alton, J. Cui, P.-P. Kung, M. D. Nambu, G. Los, S. L. Bender, B. Mroczkowski, J. G. Christensen, *Cancer Res.* **2007**, *67*, 4408.

